

## Valence-band spectra of BEDT-TTF and TTF-based magnetic charge-transfer salts

E. Z. Kurmaev,<sup>1</sup> A. Moewes,<sup>2</sup> S. G. Chiuzbian,<sup>3</sup> L. D. Finkelstein,<sup>1</sup> M. Neumann,<sup>3</sup> S. S. Turner,<sup>4</sup> and P. Day<sup>1</sup><sup>1</sup>*Institute of Metal Physics, Russian Academy of Sciences-Ural Division, 620219 Yekaterinburg, GSP-170, Russia*<sup>2</sup>*Department of Physics and Engineering Physics, University of Saskatchewan, 116 Science Place, Saskatoon, Saskatchewan S7N 5E2, Canada*<sup>3</sup>*Universitat Osnabrück, Fachbereich Physik, D-49069 Osnabrück, Germany*<sup>4</sup>*Davy Faraday Research Laboratory, The Royal Institution of Great Britain, 21 Albemarle Street, London, W1X 4BS, United Kingdom*

(Received 10 September 2001; revised manuscript received 21 March 2002; published 29 May 2002)

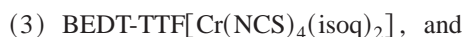
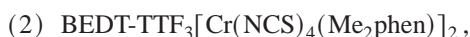
The electronic structure of BEDT-TTF bis(ethylenedithio)tetrathiafulvalene, and TTF, tetrathiafulvalene, based ferrimagnetic insulating and paramagnetic semiconducting charge-transfer salts have been studied by x-ray emission spectroscopy (XES) and photoelectron spectroscopy (XPS). The counterions for the salts are the *d*-transition-metal complex anions  $[\text{Cr}(\text{NCS})_4(\text{phen})]^-$ ,  $[\text{Cr}(\text{NCS})_4(\text{Me}_2\text{phen})]^-$  and  $[\text{Cr}(\text{NCS})_4(\text{isoq})_2]^-$  where  $\text{Me}_2\text{phen} = 4, 7$ -dimethyl-1, 10-phenanthroline,  $\text{phen} = 1, 10$ -phenanthroline, and  $\text{isoq} = \text{isoquinoline} = \text{C}_9\text{H}_7\text{N}$ . The distribution of partial and total density of states was determined by comparing the XES spectra of the constituents (carbon and nitrogen  $K\alpha$  and Cr  $L_{2,3}$ ) with XPS valence-band spectra on the binding-energy scale. Splitting in the XPS N  $1s$  and S  $2p$  spectra was attributed to contributions from nonequivalent atoms, i.e., N in the NCS and phen based ligands, S in NCS and BEDT-TTF. Cr  $L$ -XES measured at the  $L_2$ -threshold display an unusually high  $L_2$  to  $L_3$  intensity ratio, which is discussed in terms of Coster-Kronig transitions and a different excitation of  $L_3$  and  $L_2$  levels at the  $L_2$  threshold.

DOI: 10.1103/PhysRevB.65.235106

PACS number(s): 78.70.En, 73.21.-b

## I. INTRODUCTION

Charge-transfer salts of organic donors such as TTF, tetrathiafulvalene, and BEDT-TTF, bis(ethylenedithio)tetrathiafulvalene, show a wide range of transport properties: from insulating and semiconducting to metallic and even superconducting.<sup>1</sup> Until recently the focus of research into these and similar salts has been solely concerned with their transport properties, although emphasis has moved to the possibility of preparing materials with mixed conducting and magnetic properties. The magnetic properties are typically introduced via anionic complexes such as  $[\text{FeCl}_4]^-$  (see Ref. 2),  $[\text{Fe}(\text{CN})_6]^{3-}$  (see Ref. 3),  $[\text{Cr}(\text{NCS})_4(\text{NH}_4)_2]^-$  (see Ref. 4), and  $[\text{Cr}(\text{C}_2\text{O}_4)_3]^{3-}$  (see Ref. 5), which contain *d*-transition elements with unpaired and localized electron density. Recently, TTF and BEDT-TTF salts of complex anions with ligands containing delocalized  $\pi$  systems have been prepared and exhibit long-range magnetic order.<sup>6,7</sup> In the present paper we report on results of the x-ray emission and photoelectron spectra measurements of four magnetic charge-transfer salts:



where the ligands and donors are given in Fig. 1. In our previous paper<sup>8</sup> x-ray emission spectroscopy was used to study the electronic structure of BEDT-TTF molecular conductors and superconductors containing paramagnetic 3*d* ions (Cr and Fe).

The lattice structures of compounds 1–3 have been determined by single-crystal x-ray diffraction.<sup>6,7</sup> The structures of compounds (1) and (3) consist of stacks of alternating TTF or BEDT-TTF cations and  $[\text{Cr}(\text{NCS})_4(\text{phen})]^-$  or  $[\text{Cr}(\text{NCS})_4(\text{isoq})_2]^-$  anions. In both salts the closest interactions between electron donor and acceptor moieties are  $S \cdots S$  atomic contacts or  $\pi$ -stacking overlap. However, there are no significant interanion or intercation contacts and, in particular, there are no  $S \cdots S$  close contacts between donors, as typically seen in highly conducting charge-transfer salts. Compound (2) has a more typical structure of alternating layers of anions and cations with numerous interaction  $S \cdots S$  contacts.

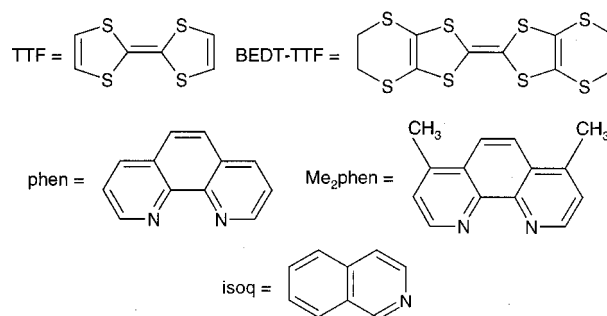
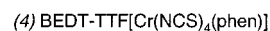
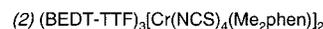
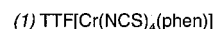


FIG. 1. Constituents of the charge transfer salts [(1)–(4)] investigated in this work.

The magnetic properties of compounds (1) and (3) are characteristic of bulk ferrimagnets exhibiting long-range magnetic order below 9 (Ref. 7) and 4.2 K (Ref. 6), respectively. By contrast, plots of magnetic susceptibility vs temperature for compounds (2) and (4) are typical of simple paramagnets. From the structural data we find that salts with magnetic order have strong cation-anion interactions whereas the paramagnetic salt (2) does not<sup>7</sup> and we can assume that compound (4), being paramagnetic, also does not. We find that an interion  $\pi$ -stacking interaction is important in promoting long-range magnetic order. Furthermore, small coercive fields have been measured for the ferrimagnetic compounds, the largest of which is 338 Oe (Ref. 6) for compound (3), BEDT-TTF[Cr(NCS)<sub>4</sub>(isoq)<sub>2</sub>].

Since the structures of compounds (1) and (3) have isolated donor molecules they predictably proved to be insulators. Compound (2) and most likely compound (4), have close  $S \cdots S$  interdonor contacts and both show semiconducting behavior. For further details of the syntheses, x-ray-diffraction studies and magnetic and transport properties, see Refs. 6 and 7.

## II. EXPERIMENT

The constituents of compounds (1)–(4) are given in Fig. 1. All charge-transfer salts were prepared by *in situ* oxidation of the relevant donor (TTF or BEDT-TTF) placed in the anode arm of a *H*-shaped electrochemical cell. The remainder of the cell was filled with a filtered solution of either [isoqH][Cr(NCS)<sub>4</sub>(isoq)<sub>2</sub>], [(C<sub>2</sub>H<sub>5</sub>)<sub>4</sub>N][Cr(NCS)<sub>4</sub>(phen)] or [(C<sub>4</sub>H<sub>9</sub>)<sub>4</sub>N][Cr(NCS)<sub>4</sub>(Me<sub>2</sub>phen)] in purified dichloromethane solvent. 1  $\mu$ A was applied across each cell for up to 1 week until suitable crystals grew on the anode. Since each cell produces just 1–3 mg of crystals, the product from several identical cells, for each salt, was used for the measurements in this work.

The nonresonant carbon and nitrogen  $K\alpha$  ( $2p \rightarrow 1s$  transition) x-ray emission spectra (XES) were recorded at the Advanced Light Source (Beamline 8.0.1) employing the soft x-ray fluorescence end station.<sup>9</sup> Photons with an energy of 300 eV (for carbon spectra) and 410 eV (for nitrogen spectra), which is well above the carbon and nitrogen  $K$  edges, were delivered to the end station via a spherical grating monochromator. The carbon and nitrogen  $K\alpha$  spectra were obtained with a 600 lines/mm, 10-m. radius grating providing an energy resolution of 0.5 eV for carbon and 0.9 eV for nitrogen. Furthermore, we have measured the chromium  $L_{2,3}$  ( $3d4s \rightarrow 2p_{1/2,3/2}$  transition) XES for the pure metal and compounds (1)–(4) in both the resonant regime (near  $L_2$  and  $L_3$  edges) and also far from thresholds (nonresonant spectra) using a 1200 lines/mm diffraction grating that provides an energy resolution of 0.8 eV. For this the excitation energy was varied from 574.3 to 620 eV.

The x-ray photoelectron spectroscopy (XPS) measurements were performed with a Physical Electronics ESCA spectrometer (PHI 5600 ci, with monochromatized Al- $K\alpha$  radiation of 0.3 eV full width at half maximum). The energy resolution of the analyzer was 1.5% of the pass energy. The estimated energy resolution was less than 0.35 eV for XPS

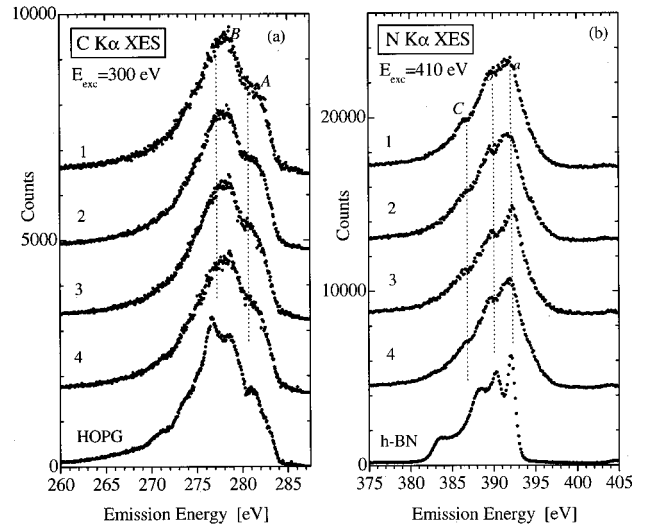


FIG. 2. Nonresonant carbon (a) and nitrogen (b)  $K\alpha$  emission spectra of compounds (1)–(4).

measurements on copper and iron sulfides. The pressure in the vacuum chamber during the measurements was below  $5 \times 10^{-9}$  mbar and before measurement the samples were fractured in the ultrahigh vacuum. All the investigations were then performed at room temperature on the freshly cleaved surface. The XPS spectra of the semiconducting sample (2) were calibrated using Au foil to obtain photoelectrons from the Au- $4f_{7/2}$  subshell where the binding energy for the Au- $4f_{7/2}$  electrons is 84.0 eV (Ref. 10). The spectra for sample 1 were calibrated by taking into account the position of the N line for the NCS ligand (398.4 eV).

## III. RESULTS AND DISCUSSION

### A. Nonresonant x-ray emission and photoelectron spectra

The nonresonant carbon and nitrogen x-ray emission spectra are recorded by exciting above the  $1s$  core ionization threshold. In nonresonant excitation, x-ray emission can be described with the emission decoupled from the excitation. That is, emission occurs when an electron undergoes a transition from an occupied valence level to fill the core hole that is created during the absorption of the incident photon. According to the dipole selection rule,  $\Delta l = \pm 1$ , the  $1s$  core level hole in carbon and nitrogen atoms can only be filled by  $p$ -valence electrons and, therefore, the intensity in the nonresonant x-ray emission spectra of carbon and nitrogen maps the  $2p$  density at each particular atomic site. In the case of chromium  $L_{2,3}$  spectra ( $3d4s \rightarrow 2p_{1/2,3/2}$  transition), the  $2p$  core-level hole is filled by  $3d4s$  valence electrons and the intensity distribution is then related to the occupied  $3d4s$  states. Since the final state of the x-ray emission process contains a hole in the valence band, one can expect the XES spectra to reflect the partial valence-orbital-resolved contribution to the single-particle spectral function<sup>11</sup> XES is thus a powerful tool for the study of highly correlated systems such as charge-transfer salts.

Figures 2(a) and 2(b) show the nonresonant carbon and nitrogen  $K\alpha$  XES of compounds (1)–(4) together with spec-

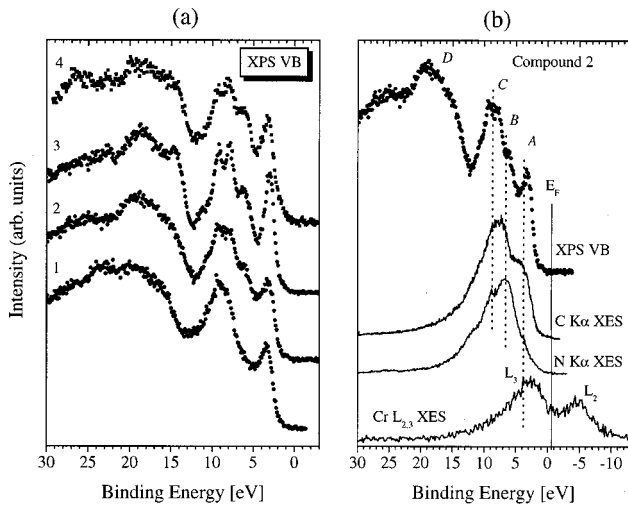


FIG. 3. (a) XPS Valence-band (VB) spectra of compounds (1)–(4) (b) Comparison of XPS VB of compound (2) with soft x-ray emission spectra of constituent atoms on common binding-energy scale.

tra of the reference samples (highly oriented pyrographite and hexagonal boronitride). Initially, we note that the carbon spectra of charge-transfer salts with different cations (TTF and BEDT-TTF) and anions ([Cr(NCS)<sub>4</sub>(phen)], [Cr(NCS)<sub>4</sub>(Me<sub>2</sub>phen)], and [Cr(NCS)<sub>4</sub>(isoq)<sub>2</sub>]) all show a similar two-peak (A-B) structure [Fig. 2(a)]. This has been observed before in spectra of conducting polymers,<sup>12,13</sup> molecular conductors and superconductors (BEDT-TTF)<sub>2</sub>Cu[N(CN)<sub>2</sub>]Br, (BEDT-TTF)<sub>2</sub>Cu(NCS)<sub>2</sub> (see, Refs. 13 and 14), (BEDT-TTF)<sub>4</sub>[(H<sub>3</sub>O)Fe(C<sub>2</sub>O<sub>4</sub>)<sub>3</sub>]·C<sub>5</sub>H<sub>5</sub>N, (BEDT-TTF)<sub>4</sub>[(H<sub>3</sub>O)Fe(C<sub>2</sub>O<sub>4</sub>)<sub>3</sub>]·C<sub>6</sub>H<sub>5</sub>CN, and (BEDT-TTF)<sub>4</sub>[(H<sub>3</sub>O)Cr(C<sub>2</sub>O<sub>4</sub>)<sub>3</sub>]·C<sub>6</sub>H<sub>5</sub>CN (see, Ref. 8) indicating that the same structure of carbon delocalized  $\pi$  states is present in all samples at the measurement temperature. Peak A corresponds to  $\pi$ -like states: peak B is due to both  $\pi$  and  $\sigma$  contributions with the  $\sigma$  states dominating.<sup>13</sup> TTF and BEDT-TTF (see Fig. 1) have a similar structural motif and so it is not surprising that the carbon spectra are rather insensitive when replacing the cation. On the other hand, it seems that carbon atoms belonging to the different anions with localized C 2*p* states exert only small perturbations on the local electronic structure of the cations at ambient temperature.

For the nonresonant nitrogen *K* $\alpha$  XES [Fig. 2(b)] it should be noted that nitrogen atoms are absent in the cation layers (Fig. 1) and belong only to the NCS, phen, and isoq ligands. Therefore these spectra characterize the local electronic structure in the anions. Since the local environment of nitrogen atoms in the phen and isoq groups is slightly different (Fig. 1) this results in a small difference between the spectrum of compound (3) and spectra of the other salts [Fig. 2(b)].

In Fig. 3 the XPS valence-band (VB) spectra recorded on all samples are presented. The spectra exhibit similar fine structures marked by peaks located at almost the same binding energies but with different relative intensities. In order to understand the origin of the different subbands, the XPS VB

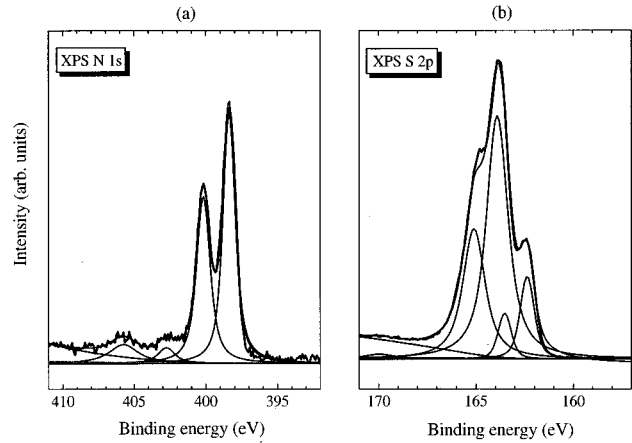


FIG. 4. XPS spectra of N 1*s* (a) and S 2*p* (b) core levels of compound (2).

of compound (2) is compared with the x-ray emission spectra of its constituents (carbon and nitrogen *K* $\alpha$  and chromium *L*<sub>2,3</sub> XES) on the binding-energy (BE) scale [see Fig. 3(b)]. In order to convert the emission energies to the binding-energy scale we have used the results of our XPS measurements of core levels:  $E_{\text{BE}}(\text{C}1s) = 285.7$  eV,  $E_{\text{BE}}(\text{N}1s) = 398.4$  eV, and  $E_{\text{BE}}(\text{Cr}2p) = 577.8$  eV. The fine structure of the XPS VB spectra in the energy range of 0–15 eV [(A–C) in Fig. 3(b)] mainly originates from the distribution of carbon 2*p* states because the shape of the C *K* $\alpha$  XES reproduces the fine structure of XPS VB in this region. Chromium 3*d*<sub>4*s*</sub> states contribute to the formation of peak A evidencing anion-cation interaction. Nitrogen 2*p* states also participate in the formation of the peak A to a small extent since these states are mainly concentrated in the vicinity of peaks B and C. We also note that subbands B and C are resolved in the nitrogen *K* $\alpha$  emission spectra due to contributions from nonequivalent nitrogen atoms having different N 1*s* binding energies [Fig. 4(a)].

In fitting the XPS spectra, a symmetrical Lorentzian line shape was assumed for all peaks since this procedure is commonly applied for insulating samples. A universal energy-loss function was taken into account for the background. This can approach Tougaard's function and also fulfils the physical constraints tending to zero at the borders zero and infinity.

Two main peaks are identified for the N 1*s* spectra of compound (2) [Fig. 4(a)]. The first N 1*s* peak corresponds to the nitrogen atoms belonging to the NCS group (8 atoms/f.u., at 398.4 eV) and the second one should be related to nitrogen atoms in the Me<sub>2</sub>phen ligand (4 atoms/f.u., at 400.2 eV). The peaks have an area ratio of 2:1.5, close to that expected from the chemical formula (2:1).

The S 2*p* spectra of compound (2) are presented in Fig. 4(b). The spectra were fitted by recognizing two discrete sulphur sites in the sample. Due to the strong S overlap in neighboring BEDT-TTF molecules, two physical constraints were used in order to facilitate resolving each line. For each sulphur site a 1.18 eV spin-orbit splitting was taken into account since the spin-orbit splitting should be compound independent. Additionally, the ratio of the areas 2*p*<sub>3/2</sub> to

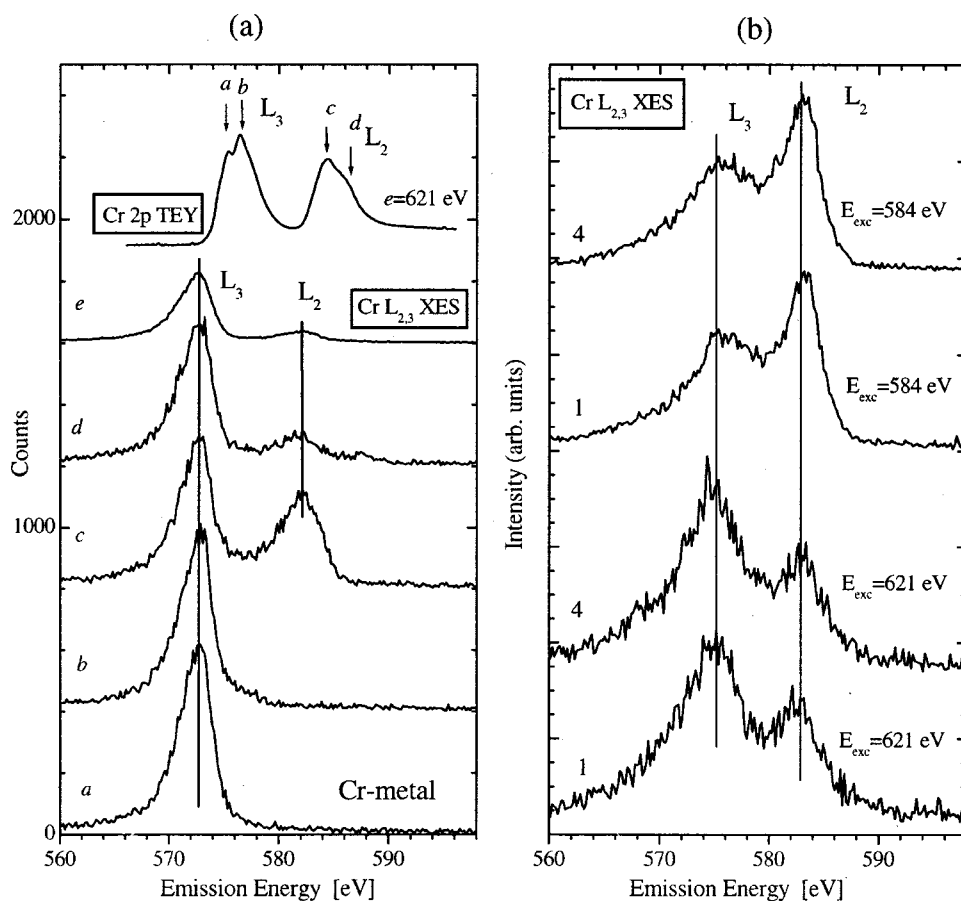


FIG. 5. Resonant and nonresonant Cr  $L_{2,3}$  XES of pure metal (a) and compounds (2) and (4) (b).

$2p_{1/2}$  was fixed to be 2.0, reflecting the occupancy of each subshell. The first two peaks in Fig. 4(b) were attributed to S  $2p_{3/2}$  and  $2p_{1/2}$  lines of the NCS ligand (8 atoms/f.u.) and the remaining peaks originate from S in BEDT-TTF (24 atoms/f.u.). The binding energies of these S  $2p_{3/2}$  lines were found to be 162.4 and 163.9 eV, respectively. The XPS N  $1s$  and S  $2p$  spectra recorded for the other compounds were found to be very similar and only differences in the relative intensities of each peak were observed, in agreement with the compound stoichiometries.

### B. Resonant x-ray emission spectra

Resonant x-ray emission spectra are measured using selective incoming photon energies near threshold. Figure 5(a) shows the resonant Cr  $L_{2,3}$  XES for the pure metal and since Cr  $L_{2,3}$  XES for compounds (1)–(4) were very similar, examples of compounds (2) and (4) are given in Fig. 5(b). Furthermore, the Cr  $2p$  x-ray-absorption spectra (XAS) measured in the total electron yield mode are found to be very similar in compounds (1)–(4) (not shown) and in the pure metal. Arrows indicate the selected excitation energies. In Fig. 5(a) the intensities of the  $L_3$  and  $L_2$  lines, i.e.,  $I(L_3)$  and  $I(L_2)$ , vary for the pure Cr metal according to the density of unoccupied states above the  $L_3$  and  $L_2$  thresholds. At the  $L_2$  threshold (labeled  $c$  in Fig. 5) the  $L_2$  level is resonantly excited whereas the  $L_3$  is excited nonresonantly, accounting for the sharp increase of  $I(L_2)/I(L_3)$  compared to complete nonresonant excitation (labeled  $d$  and  $e$ ).

For nonresonant Cr  $L$ -emission spectra of compounds (2) and (4) [Fig. 5(b)] the ratio  $I(L_2)/I(L_3)$  is estimated to be almost four times higher than for the pure metal [Fig. 5(a)]. This is mainly due to the high probability of  $L_2 \rightarrow L_3$  Coster-Kronig transitions in Cr metal and to some extent due to smaller magnetic contributions to  $I(L_2)/I(L_3)$  for pure  $3d$  metals.<sup>15</sup> Also when the excitation energy becomes equal to the energy of  $L_2$  XAS the  $I(L_2)/I(L_3)$  intensity ratio sharply increases for the investigated salts [Fig. 5(b)] as well as in the pure metal [Fig. 5(a)] by approximately four times. We attribute this to the different probabilities for  $L_2$  absorption and  $L_3$  ionization for resonant and nonresonant excitation.

The XPS Cr  $3s$  spectra of compounds (1)–(4) are plotted in Fig. 6 and the  $s$ -level line shape is clearly split by 3.8–3.9 eV. The splitting correlates with the local magnetic moments<sup>16</sup> and confirms the spin polarization of Cr centers. Unfortunately, it is not possible to separate magnetic contributions of the Cr ion and the organic donors using bulk magnetic measurements. However, the total magnetic moments per Cr center at 300 K measured with a superconducting quantum interference design, MPMS-7 magnetometer for compounds (1)–(4) are 4.21, 4.06, 4.25, and 4.18  $\mu_B$ , respectively. For the insulating samples (1) and (3) the donors are isolated and so at 300 K the unpaired electron density is likely to be localized at the individual donor molecules. Since electron paramagnetic resonance spectroscopy<sup>1</sup> gives Landé  $g$  factors close to the free electron value, for salts of this type, there is little orbital contribution to their magnetic

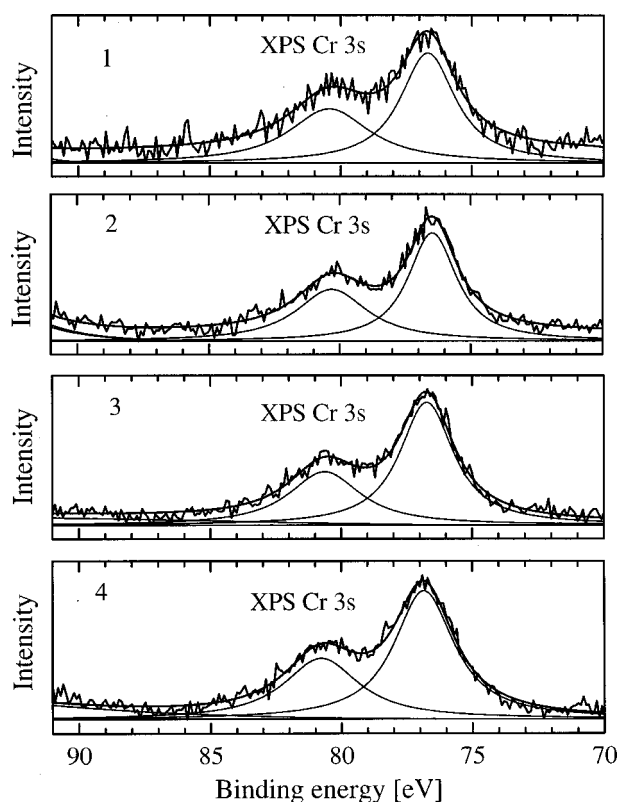


FIG. 6. XPS Cr 3s spectra of compounds (1)–(4).

moment. Therefore, if one assumes that the donor magnetic contributions to compounds (1) and (3) are equivalent to the magnetic moment of a free electron then the measured contributions due to Cr ions alone are  $3.84$  and  $3.88 \mu_B$ , respectively. These values are close to the spin only value for  $\text{Cr}^{3+}$  ( $3.87 \mu_B$ ). For compound (2) the magnetic contribution from the donors should be less than the maximum for 1.5 electrons per Cr center, since the unpaired electrons associated with BEDT-TTF are not localized, but are associated with an electronic band. Indeed one were to remove the full maximum donor contribution from the measured susceptibility this

would leave just  $3.46 \mu_B$  assigned to the Cr center, which is far too a low. For compound (4) it has been difficult to estimate the ratio of donors to Cr ions since structural information is not yet available, although a similar argument to that for compound (2) is likely. It should be noted that similar energy splitting in the Cr 3s XPS (4.1 eV) is observed for  $\text{LiCrO}_2$  (Ref. 16) where the effective magnetic moment is estimated to be  $3.71 \mu_B$ .

## CONCLUSION

We have studied the electronic structure of some BEDT-TTF and TTF-based magnetic charge-transfer salts with Cr-containing counter ions using x-ray emission and x-ray photoelectron spectroscopy. A comparison of x-ray emission spectra with XPS valence-band spectra on the binding-energy scale allowed determination of the distribution of partial and total density of states in the valence band. We found a splitting of XPS N 1s and S 2p core levels, which is attributed to nonequivalent atoms in the anion and cation molecules (N in either NCS or phenanthroline ligands; S in either NCS or BEDT-TTF). We further discussed the anomalous high ratios of  $L_2$  to  $L_3$  intensities in resonant and non-resonant Cr  $L_{2,3}$  emission in terms of Coster-Kronig transitions and different excitation of  $L_2$  and  $L_3$  levels at  $L_2$  threshold.

## ACKNOWLEDGMENTS

This work was supported by the Russian Foundation for Basic Research (Projects Nos. 00-15-96575 and 02-02-16674), the Russian State Program on Superconductivity, the NATO Collaborative Linkage Grant No. (PST.CLG.978044), and the National Sciences and Engineering Research Council (NSERC). Funding by the Deutsche Forschungsgemeinschaft through the Graduiertenkolleg ‘‘Mikrostruktur oxidischer Kristalle’’ and the UK Engineering is gratefully acknowledged. The Advanced Light Source at Lawrence Berkeley National Laboratory is supported by the U.S. Department of Energy (Contract No. DE-AC03-76SF00098).

- <sup>1</sup>J. M. Williams, J. R. Ferraro, R. J. Thorn, K. D. Karlson, U. Geiser, H. H. Whang, A. M. Kini, and M. H. Whangbo, *Organic Superconductors (including Fullerenes) Synthesis, Structure, Properties and Theory* (Prentice-Hall, New York, 1992).
- <sup>2</sup>H. Kobayashi, T. Naito, A. Sato, K. Kawano, A. Kobayashi, H. Tanaka, T. Saito, M. Tokumoto, L. Brossard, and P. Cassoux, *Mol. Cryst. Liq. Cryst. Sci. Technol., Sect. A* **284**, 61 (1996).
- <sup>3</sup>P. Le Magueres, L. Ouahab, N. Conan, D. J. Gomez-Garcia, P. Delhaes, J. Even, and M. Bertault, *Solid State Commun.* **97**, 27 (1996).
- <sup>4</sup>C. J. Kepert, M. Kurmoo, M. R. Truter, and P. Day, *J. Chem. Soc. Dalton Trans.* **1997**, 607 (1997).
- <sup>5</sup>L. Martin, S. S. Turner, P. Day, F. E. Mabbs, and E. J. L. McInnes, *Chem. Commun. (Cambridge)* **1997**, 1367 (1997).
- <sup>6</sup>S. S. Turner, C. Michaut, S. Durot, P. Day, T. Gelbrich, and M. B.

- Hursthouse, *J. Chem. Soc. Dalton Trans.* **2000**, 905 (2000); F. Setifi, S. Golhen, L. Ouahab, S. S. Turner, and P. Day, *Cryst. Eng. Comm.* **2002**, 1 (2002).
- <sup>7</sup>S. S. Turner, D. Le Pevelen, P. Day, and K. Prout, *J. Chem. Soc. Dalton Trans.* **2000**, 2739 (2000); S. S. Turner, P. Day, T. Gelbrich, and M. B. Hursthouse, *J. Solid State Chem.* **159**, 385 (2001). An article detailing the synthesis and physical properties of compound (2) is in preparation.
- <sup>8</sup>E. Z. Kurmaev, V. R. Galakhov, A. Moewes, S. Shimada, K. Endo, S. S. Turner, P. Day, R. N. Lyubovskaya, D. L. Ederer, and M. Iwami, *Phys. Rev. B* **62**, 11 380 (2000).
- <sup>9</sup>J. J. Jia, T. A. Callcott, J. Yurkas, A. W. Ellis, F. J. Himpsel, M. G. Samant, J. Stöhr, D. L. Ederer, J. A. Carlisle, E. A. Hudson, L. J. Terminello, D. K. Shuh, and R. C. C. Perera, *Rev. Sci. Instrum.* **66**, 1394 (1995).

- <sup>10</sup>J. F. Moulder, W. F. Stickle, P. E. Sobol, and K. D. Bomben, *Handbook of X-ray Photoelectron Spectroscopy* (Perkin-Elmer, Eden Prairie, Minnesota, 1992).
- <sup>11</sup>U. von Barth and G. Grossmann, *Phys. Rev. B* **25**, 5150 (1982).
- <sup>12</sup>E. Z. Kurmaev, M. I. Katsnelson, A. Moewes, M. Magnuson, J.-H. Guo, S. M. Butorin, J. Nordgren, D. L. Ederer, and M. Iwami, *J. Phys.: Condens. Matter* **13**, 3907 (2001).
- <sup>13</sup>J. Guo and J. Nordgren, *J. Electron Spectrosc. Relat. Phenom.* **110-111**, 105 (2000).
- <sup>14</sup>E. Z. Kurmaev, S. N. Shamin, Y.-N. Xu, W. Y. Ching, A. Moewes, D. L. Ederer, E. B. Yagubskii, and N. D. Kushch, *Phys. Rev. B* **60**, 13 169 (1999).
- <sup>15</sup>V. I. Grebennikov, V. R. Galakhov, L. D. Finkelstein, N. A. Ovechkina, E. Z. Kurmaev, and A. Moewes, *Russian J. Solid State Phys.* (to be published).
- <sup>16</sup>V. R. Galakhov, M. Neumann, and N. A. Ovechkina (unpublished).